Predicting the Extreme-UV and Lyman-α Fluxes Received by Exoplanets from their Host Stars

Jeffrey L. Linsky[1], Kevin France[2], Thomas Ayres[2]

[1] *JILA, University of Colorado and NIST, Boulder, CO 80309-0440 USA*

[2] *CASA, University of Colorado, Boulder, CO 80309-0593 USA*

Abstract.

Extreme-UV (EUV) radiation from the chromospheres, transition regions, and coronae of host starsspectral types F, G, K, and M) ionize and heat the outer atmospheres of exoplanets leading to mass loss that is observed during transits and can change the exoplanet's atmosphere. Lyman-αemission from host stars controls the photochemistryn the upper layers of planetary atmospheres by photodissociating important molecules including H_2O, CO_2, CH_4, thereby increasing the oxygen and ozone mixing ratios important for habitability. Both the EUVand strong Lyman-α radiation are largely absorbed by the interstellar medium and must be reconstructed or estimated to understand the radiation environment of exoplanets. In two recent papers, Linsky et al. (2013) and Linsky et al. (2014), we have presented robust methods for predicting the intrinsic Lyman-α and EUV fluxes from main sequence cool stars. Solar models and satellite observations (HST, FUSE, and EUVE) provide tests for the feasibility of these methods.

1. Estimating the Host Star's EUV Flux

The solar EUV spectrum (Figure 1) contains emission features produced in the chromosphere (e.g., H I Lyman and He I continua) and emission lines from the transition region and corona. Late-type stars should contain the same features, but the ISM absorbes all of the 40–91.2 nm flux and most of the flux at shorter wavelengths. The EUVE satellite obtained fluxes at $\lambda < 40$ nm for a few nearby stars.

Semi-empirical models of portions of the solar atmosphere with different heating rates (e.g., Fontenla et al. 2014) show that the EUV to Lyman-α flux ratios vary smoothly with

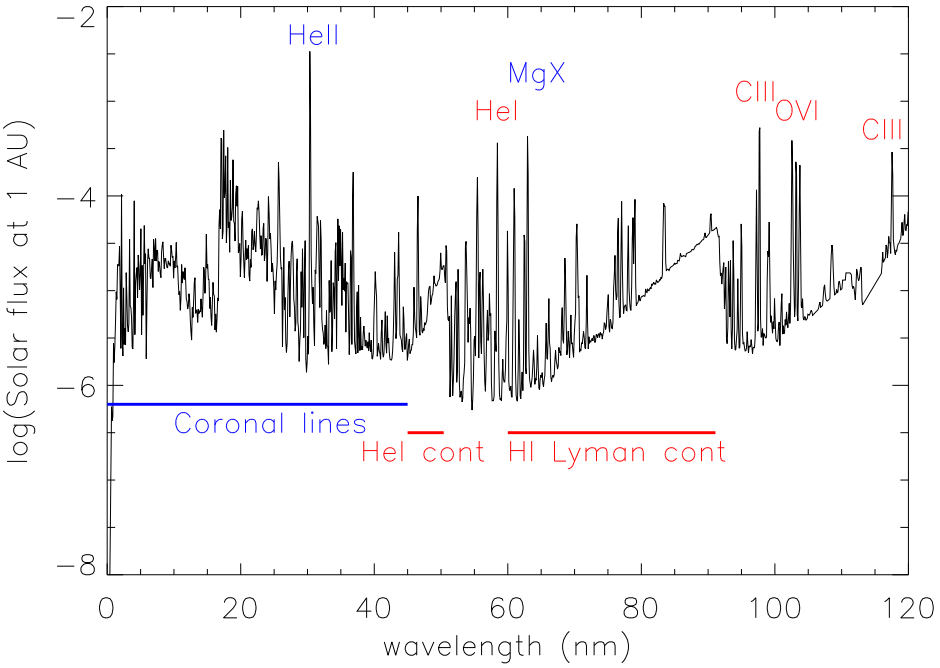

Figure .1: The Solar Irradiance Reference Spectrum (SIRS) obtained at solar minimum (March–April 2008) (Woods et al. 2009). Flux units are $Wm^{-2}nm^{-1}$ at 1 AU.

the Lyman-α flux. We show these flux ratios in different wavelength bands in Figures 2-4. These figures also show the available flux ratios obtained from the EUVE satellite and reconstructed Lyman-α fluxes. These figures show that: the EUVE/Lyman-α flux ratios have a linear dependence on the Lyman-α flux for F-K stars and the ratios are constant for the M stars. The flux ratios for the F-K stars are similar to the solar flux ratios for the same Lyman-α fluxes.

Figure 5 shows the solar EUV/Lyman-α flux ratios for the 40–70 nm region where there are no stellar observations for comparison. Not shown are solar flux ratio plots for the 70–91.2 nm region and the 91.2–117 nm region where there is good agreement with FUSE satellite observations of 5 stars.

2. Estimating the Star's Lyman-α Flux

Photodissociation of H_2O, CH_4, CO_2 and other important molecules in exoplanet atmospheres is controlled by radiation from the host star at wavelengths shortward of 170 nm. The brightest emission line in this spectral region, the H I Lyman-α line at 121.6 nm, contains as much flux as the 116–169 nm spectrum of the Sun and as much flux as the whole ultraviolet spectrum (116–305 nm) of M dwarfs (France et al. 2013). Reconstructing the intrinsic Lyman-α line flux to correct for interstellar H I absorption is feasible for nearby stars but requires high-resolution Lyman-α line spectra with the HST/STIS instrument (see Wood et al. 2005; France et al. 2013).

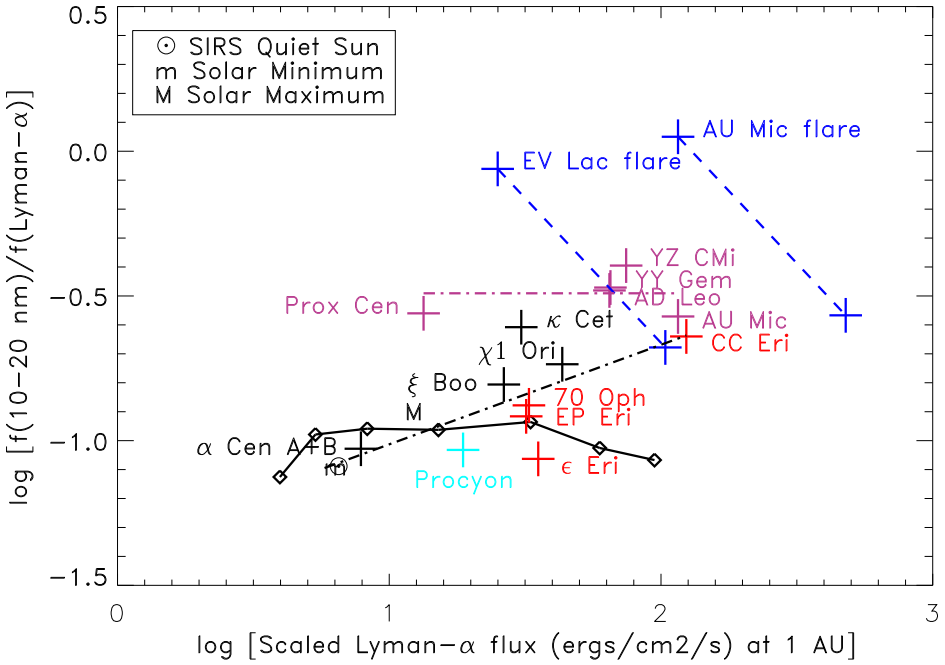

Figure .2: Ratios of the 10–20 nm intrinsic flux (corrected for interstellar absorption) divided by the reconstructed Lyα flux vs. the reconstructed Lyα flux at 1 AU scaled by the ratio of stellar radii squared. The solid line-connected diamonds are the flux ratios in this passband for the Fontenla et al. (2014) semiempirical models 13x0 to 13x8 (from left to right). Flux ratios for one F star (cyan), four G stars (black), four K stars (red), and five M stars (plum) based on *EUVE* spectra are shown as ±15 error bar symbols. The dash-dot (black) line is the least-squares fit to the solar and F, G, and K star ratios. The plum dash-dot line is the mean of the M star ratios excluding the EV Lac flare and AU Mic flare data. Flux ratios for EV Lac and AU Mic during flares (blue) are plotted two ways. The upper left symbols are ratios of EUV flare fluxes to quiescent Lyα fluxes. Dashed lines extending to the lower right indicate the ratios for increasing Lyα flux. The symbols at the lower end of the dashed lines are ratios obtained using the most likely values of the Lyα fluxes during flares.

From Wood et al. (2005) and France et al. (2012), we now have intrinsic Lyman-α fluxes for 45 F5 V to M5 V stars. We first study how accurately one can estimate the intrinsic Lyman-α flux from the $T_{\rm eff}$ of a star. Figure 6 shows that the range in intrinsic Lyman-α flux is more than an order of magnitude at a given $T_{\rm eff}$. We can narrow this range considerably by including an activity indicator such as the rotation period ($P_{\rm rot}$). The scatter about least-squares fit lines is generally less than a factor of 2 but larger for M dwarfs. The scatter is further reduced by plotting the Lyman-α flux in the habitable zone rather than at a standard distance of 1 AU. Note that the intrinsic Lyman-α flux in the habitable zone for M dwarfs is about 10 times larger than for the Sun.

One can obtain more accurate estimates of the intrinsic Lyman-α flux by comparison to other emission lines formed in the stellar chromosphere and transition region. Figure 7 shows the ratio of Lyman-α to the C IV 154.8+155.0 nm lines. If changes in the magnetic heating

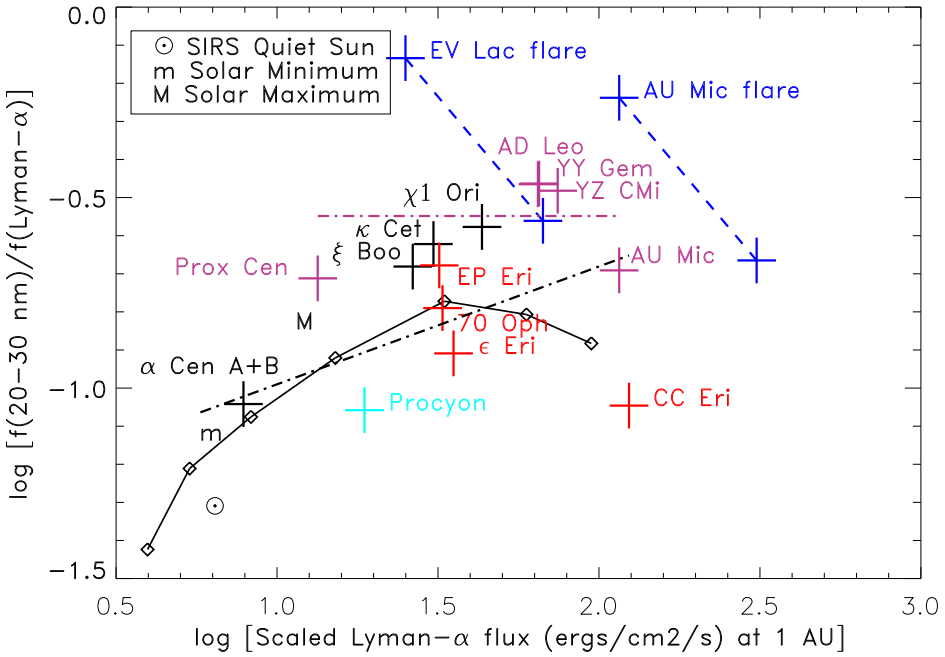

Figure .3: Same as Figure 2 except for the 20–30 nm wavelength interval.

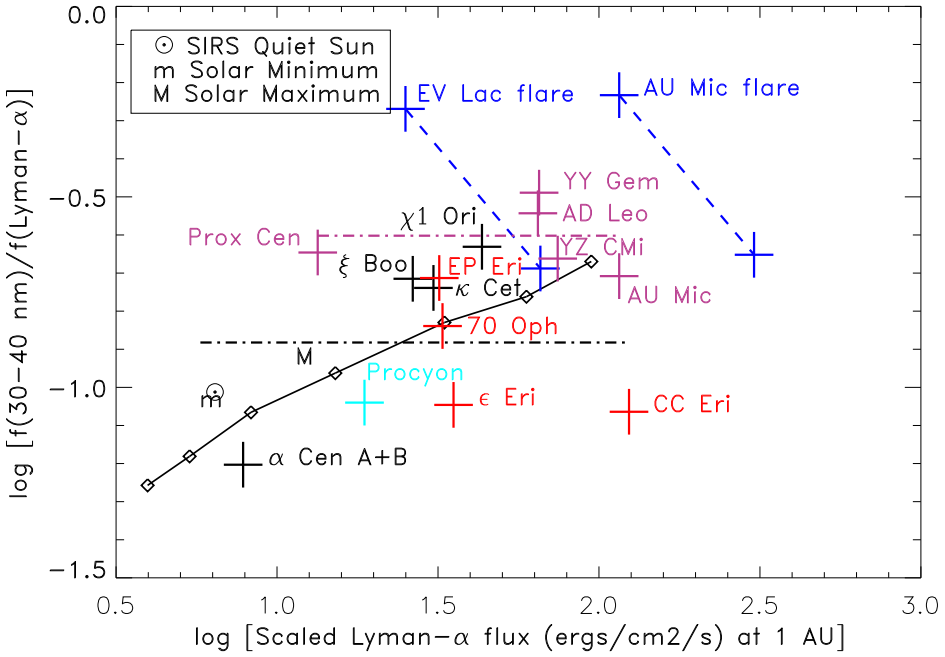

Figure .4: Same as Figure 2 except for the 30–40 nm wavelength interval.

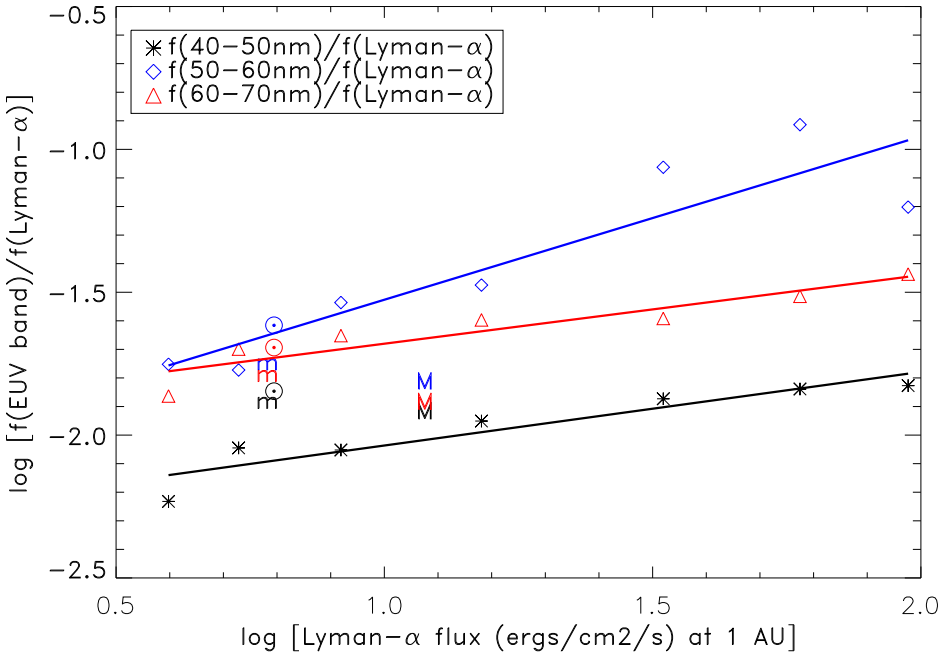

Figure .5: Same as Figure 2 except for the 40–50 nm, 50–60 nm, and 60–70 nm wavelength bands.

rate in a stellar chromosphere mainly alter the densities but not the thermal structure, then we anticipate that line ratios will depend gradually on line flux with little scatter about the least-squares fit lines. Figure 7 shows this to be the case for F5 V to K5 V stars but not the M stars. We believe that the large scatter for the variable M stars is due to observations of Lyman-α and the UV lines at different times. We find similar results when plotting ratios of Lyman-α to lines of C II, O I, and Mg II.

Figure 8 shows the correlation of the intrinsic Lyman-α flux with the flux of the Ca II H and K lines formed in the lower chromosphere. This correlation provides a tool for inferring the flux of the strongest ultraviolet emission line from optical spectra. Other UV emission lines and the EUV flux in different wavelength bands can then be inferred indirectly from the Ca II emission line fluxes.

3. Future Work

Our objective is to provide accurate fluxes required for computing the photochemistry and mass loss from exoplanet atmospheres. The reconstructed Lyman-α fluxes in the Linsky et al. (2013) paper are being used to construct new atmosphere models of terrestrial and mini-Neptune planets by Rugheimer et al. and by Miguel et al. We are also writing a paper that will present the complete spectra (X-rays to IR) for a representative sample of K and M stars including exoplanet host stars.

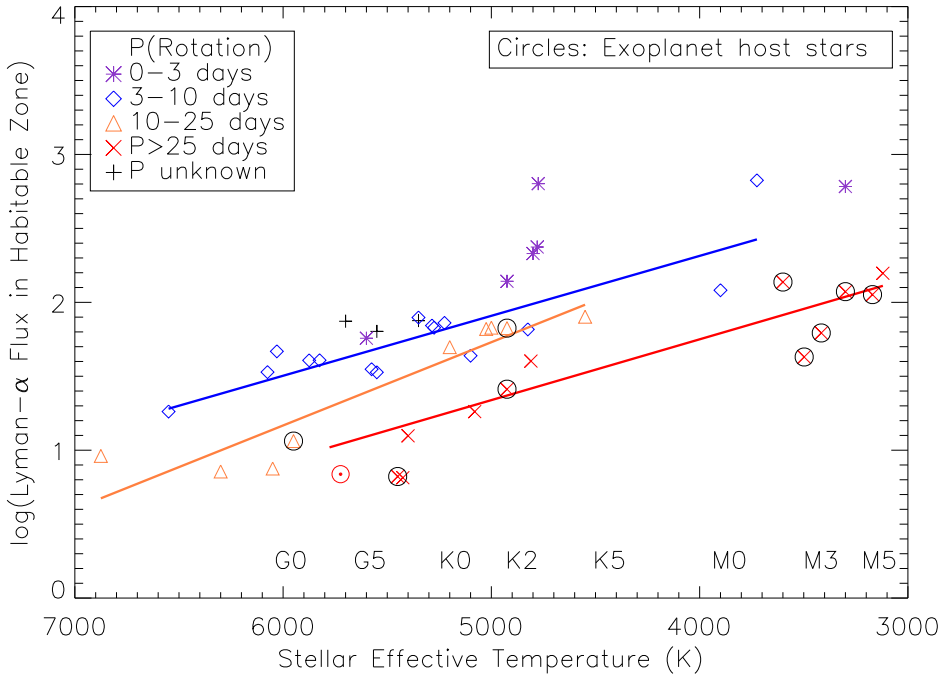

Figure .6: Lyman-α flux at 1 AU vs. stellar effective temperature. The stars are grouped according to stellar rotation period: ultrafast rotators ($P_{\rm rot} < 3$ days), fast rotators (3–10 days), moderate rotators (10–25 days), and slow rotators (> 25 days). Rotation period is a rough measure of the magnetic heating rate in the star's chromosphere and corona. Host stars of exoplanets are circled and the quiet Sun is marked as a circled dot. Least-squares fit lines are shown for the fast, moderate, and slow rotators.

Acknowledgements. This work is supported by grants from the Space Telescope Science Institute to the University of Colorado. STScI is operated by the Association of Universities for Research in Astronomy, Inc., under NASA contract NAS 5-26555.

References

Fontenla, J. M., Landi, E., Snow, M., & Woods, T. 2014, Solar Phys., 289, 515

France, K., Linsky, J. L., Feng, T., Froning, C. S., & Roberge, A. 2012a, ApJ, 750, 32

France, K., Froning, C. S., Linsky, J. L., Roberge, A., Stocke, J. T., Yian, F., Bushinsky, R., Désert, J.-M., Mauas, P., Vieytes, M., & Walkowitz, L. M. 2013, ApJ, 763, 149

Linsky, J. L., France K., & Ayres, T. R. 2013, ApJ, 766, 69

Linsky, J. L., Fontenla, J., & France, K. 2014, ApJ, 780, 61

Wood, B. E., Redfield, S., Linsky, J. L., Müller, H.-R., & Zank, G. P. 2005, ApJS, 159, 118

Woods, T. N., et al. 2009, J. Geophys. Res., 36, L01101

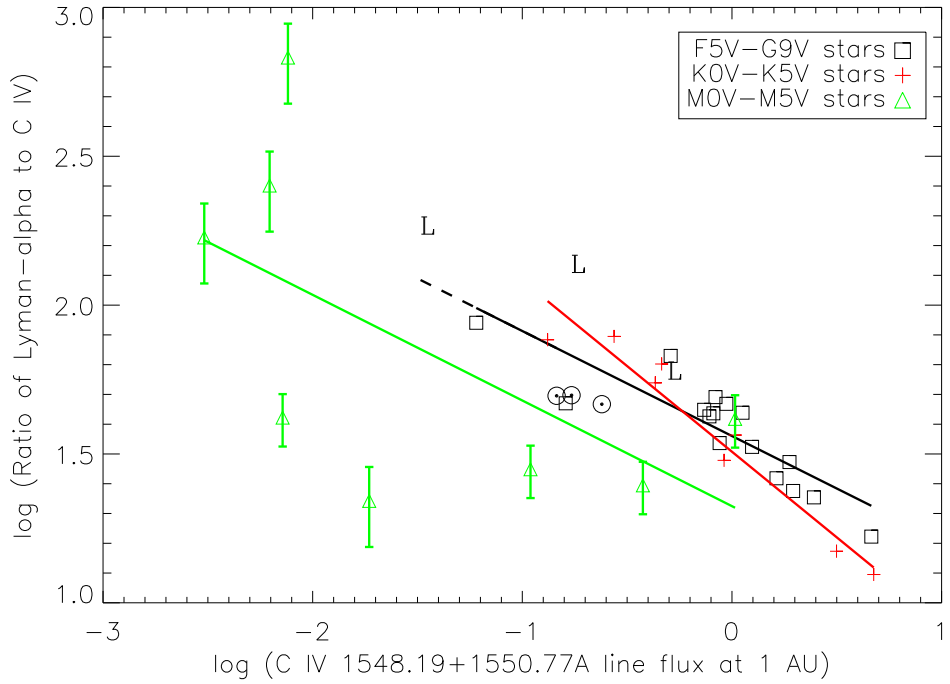

Figure .7: Plot of the ratio of the Lyman-α to C IV 154.8+155.0 nm line flux vs. the C IV line flux at 1 AU. Included are stars between spectral types F5 V and M5 V, divided into three spectral type bins, the quiet Sun and the active Sun at two different times. The solar data are indicated by Sun symbols, and the L symbol refers to a star with low metal abundance [Fe/H] < -0.30. The solid lines are least-squares fits for each spectral type bin excluding the L stars and the Sun. The ratio for α Cen A is closest to the solar ratios. The errors bars are 20% for stars using the Wood et al. (2005) correction for missing Lyman-α flux or 30% for stars using the France et al. (2012) correction for missing Lyman-α flux.

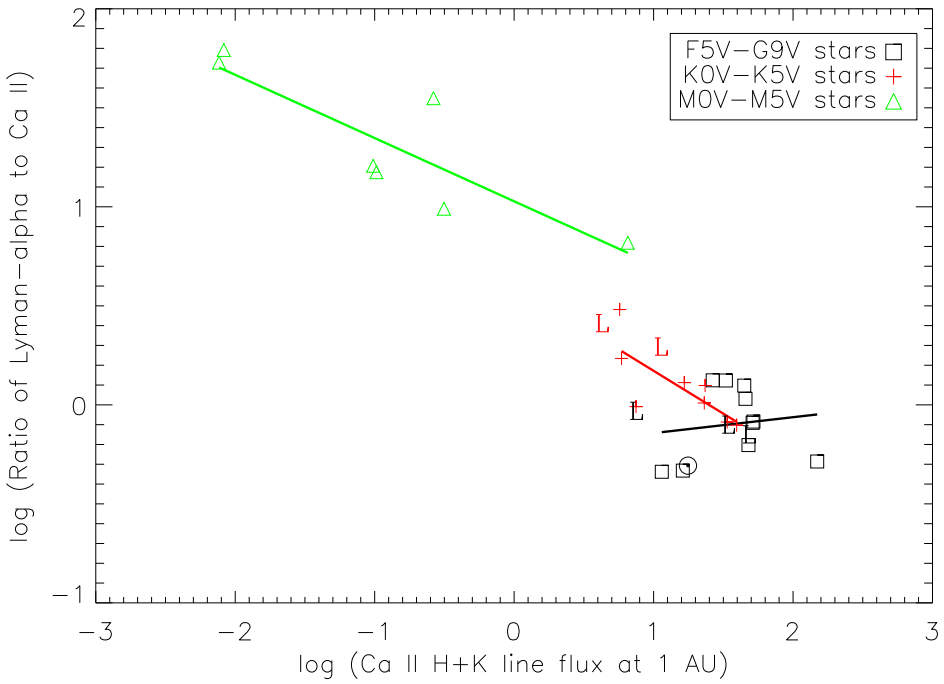

Figure .8: Plot of the Lyman-α to Ca II 3933 + 3968 Å line flux ratio vs. the Ca II line flux at 1 AU for the M0 to M5 stars. The solar data are indicated by the Sun symbol, and the L symbol refers to a star with low metal abundance [Fe/H] < -0.30. The solid lines are least-squares fits for each spectral type bin excluding the L stars and the Sun.